

## CHEMICAL AND PHYSICAL PROPERTIES OF PALEOZOIC POTASSIUM BENTONITES FROM KINNEKULLE, SWEDEN

ANN MARIE BRUSEWITZ

Geological Survey of Sweden, Box 670, S-751 28 Uppsala, Sweden

**Abstract**—The <1- $\mu\text{m}$  fraction of 17 bentonite samples from Kinnekulle, southwest Sweden, were studied by chemical analysis, X-ray powder diffraction, and cation-exchange capacity. The bentonites are interbedded with undeformed, flat-laying Ordovician and Silurian sediments and were formed by the transformation of volcanic ash (dated at about 450 Ma) into smectite, which later converted to mixed-layer illite/smectite (I/S). The reaction, possibly driven by heat from an overlying diabase intrusion (about 300 Ma), stopped at different stages of conversion, as evidenced by the I/S which ranges in composition from 60 to 10% smectite layers. A 2-m-thick bed shows zonation, with decreasing smectite proportions towards the upper contact. The zonation is not symmetrical towards the lower contact. In thin beds the illite proportion is higher and the regularity of ordering is inversely proportional to the thickness of the bed. K:Sr and K:Rb ratios follow the illite pattern; the ratios are highest at the contact and in thin beds. The inhibiting effect of Ca and Mg on the smectite-to-illite conversion probably was the cause of less-reacted smectite in the center of the thick bed.

**Key Words**—Bentonite, Igneous intrusion, Illite, Interstratification, Potassium, Smectite, X-ray powder diffraction.

### INTRODUCTION

Middle Ordovician and Silurian sedimentary rocks in the Kinnekulle region, southwest Sweden, are interbedded with K-bentonites that contain a series of mixed-layer illite/smectites (I/S) which show a wide range of systematic changes in the proportion of smectite layers. The bentonites occur in flat-laying sedimentary rocks shielded from erosion by a cap rock of Permian-Carboniferous diabase. The first comprehensive description of the bentonites was reported from a drill core through the Paleozoic sediments at Kullatorp, on the western slope of Kinnekulle, and from outcrops at Stora Mossen, on the eastern slope (Waern *et al.*, 1948). Byström (1954, 1956) showed the bentonites to be of two types: that from the two thinner beds (A-beds) contained 5%  $\text{K}_2\text{O}$  and about 60% illite layers in the I/S; the other from a 2-m-thick bed (B-bed) just below the A-beds contained 2.5%  $\text{K}_2\text{O}$  and about 20% illite layers in the I/S. The samples then available gave no information on I/S variations within the thick bed. Thinner beds (C-beds) below the B-bed also were reported to contain high percentages of illite layers in the I/S.

Byström (1954, 1956) reported that the bentonites were derived from volcanic ash falls, but for the successive change to K-bentonites, the source of K remained a problem—sea water, volcanic glass, or some other source. It was not initially determined whether the I/S minerals were present only in a few rational proportions of smectite and illite layers, or as a continuous range. In addition to the I/S proportions mentioned above, Weaver (1953), in his study of Ordovician K-bentonites from North America, found 80%

illite layers in the I/S. A detailed study of the thick bentonite bed was initiated to illuminate these problems, and a systematic sampling was made by the present author in 1955. Some of these samples were also used by Hower and Mowatt (1966), Reynolds and Hower (1970), and Velde and Brusewitz (1982). Since the initial Kinnekulle study, many publications on I/S in bentonites of different ages have been made (e.g., Šrodón, 1976; Snäll, 1977; Schultz, 1978; Inoue *et al.*, 1978; Pevear *et al.*, 1980; Huff and Türkmenöglü, 1981; Nadeau and Reynolds, 1981; Altaner *et al.*, 1984). In relation to many of the above bentonites, the Kinnekulle materials are unique in that no thrusting or re-deposition has occurred and samples with a wide range of I/S compositions can be collected from a single locality.

The aim of the present study is to document the I/S minerals from several levels in a 2-m-thick B-bed and from the thinner beds and to draw conclusions regarding the smectite-to-illite conversion process. The methods employed were X-ray powder diffraction, chemical analysis, and cation-exchange capacity. K/Ar age determinations were also made, but for the most part will be reported elsewhere.

### GEOLOGIC SETTING

The sedimentary rocks at Kinnekulle were not subjected to major tectonic activity and are flat-laying. The Kinnekulle diabase cap today covers an area of 0.4  $\text{km}^2$  and is about 30 m thick. According to Sundius it had a wider extension (see Johansson *et al.*, 1943), possibly being connected to the diabase intrusives in the Billingen area, 30 km to the southeast. The latter

Table 1. Samples studied from Kinnekulle, southwestern Sweden.<sup>1</sup>

Sample	Depth in core (m)	Bed thickness (cm)	Comments
<b>Kullatorp core</b>			
<b>Silurian samples</b>			
K6	6.35	1	
K13	13.23	1	
K15	15.68	6	
K17	17.70	1-2	
<b>Ordovician samples</b>			
K71	71.52	30	Top of bed
K72	72.75	90	Middle of bed
K74	74.52	15	Middle of bed
K78	78.61	3	
B-bed	67.35-69.05	170-180	Not sampled in core
Interval from top of bed (cm)			
<b>Stora Mossen</b>			
B-bed		180	
B31		0-5	
B32		0-5	
B33		9-30 (finer parts)	
B34		9-30 (coarser parts)	
B35		30-37	
B36		45-60	
B37		60-70	
B38		75-80	
B39		110	

<sup>1</sup> The Kullatorp core was drilled on the western slope of Kinnekulle. The levels of sampling were taken from the description of the core (Waern *et al.*, 1948), the exact position not being possible to define in the present state of the core. The B-bed was sampled at Stora Mossen on the eastern slope, where the bentonite was mined by Skånska Cement Co. in the 1940s.

intrusives were dated by Priem *et al.* (1968) by the K/Ar method at  $287 \pm 15$  Ma.

Bentonites occur in both Silurian and Middle Ordovician marine rocks. Thorslund placed the latter in the Caradocian, lower Chasmops series (see Waern *et al.*, 1948). In a more recent stratigraphic determination, the bentonites were placed within the Skagen and Dalby formations (limestone), with the boundary between these units at the top of the B-bed (Skoglund, 1963; Jaanusson, 1964). The volcanic ash fall that was the precursor of this bed was dated by the K/Ar technique on sanidine phenocrysts at  $444 \pm 20$  Ma (Byström-Asklund *et al.*, 1961). Recently, biotites from the same fractionated material were dated by the <sup>40</sup>Ar-<sup>39</sup>Ar method at 455 Ma (Kunk *et al.*, 1984).

Figure 1 shows a schematic section of the Kinnekulle strata. The Ordovician bentonites occur with grey and black shale, calcareous mudstone, and limestone containing glauconite in the upper part. Strata adjacent to the bentonite beds are typically cherty. Bentonites are

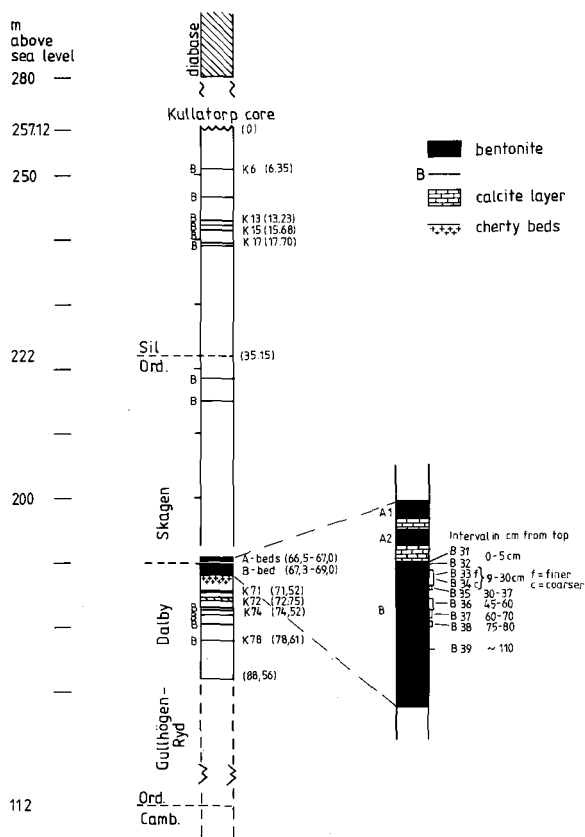


Figure 1. Schematic section of Kinnekulle, showing position of samples investigated in the study. Stora Mossen profile enlarged (modified after Thorslund in Waern *et al.*, 1948).

abundant, but the most interesting one is the 2-m-thick B-bed. Above this bed, separated by a 20-cm-thick calcite layer, are two thinner A-beds, A1 and A2, each about 15 cm thick. Below the B-bed are nearly 20 C-beds, of variable thicknesses, some as thick as 90 cm. The bentonites consist mainly of I/S, but phenocrysts are present in varying amounts. In the B-bed quartz varies from 5 to 20%, biotite and sanidine from 2 to 5%, and plagioclase phenocrysts (strongly kaolinized) from 5 to 10%. In addition, pyrite and other phenocrysts are present in subordinate amounts (Byström, 1956).

The Silurian bentonites are interbedded with grey and red mudstone interbedded with black shales (Waern *et al.*, 1948). All Silurian bentonites are thin, mostly less than 2 cm thick.

## EXPERIMENTAL

### Sampling

The samples studied are listed in Table 1 and marked in Figure 1. From the Kullatorp core four samples were selected from Silurian bentonites and four from the

Table 2. Chemical analyses (wt. %) and cation-exchange capacity (CEC) of Kinnekulle bentonites, <1- $\mu$ m fraction.

	Sample																
	K6	K13	K15	K17	B31	B32	B33	B34	B35	B36	B37	B38	B39	K71	K72	K74	K78
SiO <sub>2</sub>	49.0	49.0	48.0	49.0	54.0	54.0	54.0	52.4	56.1	53.6	53.4	52.5	52.9	52.6	53.1	52.2	50.5
Al <sub>2</sub> O <sub>3</sub>	27.1	26.4	28.3	25.9	21.0	21.6	20.0	20.2	20.0	20.6	19.9	19.9	19.7	22.5	22.3	22.3	24.0
Fe <sub>2</sub> O <sub>3</sub>	3.4	2.5	2.5	2.5	1.6	1.6	1.8	2.1	1.8	2.0	2.0	2.1	2.2	2.0	2.1	2.5	1.6
FeO	1.06	1.00	0.64	0.89	0.70	0.64	0.71	0.70	0.94	1.02	0.88	0.88	0.75	0.72	0.82	0.83	0.87
MgO	2.45	2.97	2.23	2.57	3.84	4.04	4.20	4.28	4.00	4.45	4.26	4.21	4.49	3.74	3.59	3.81	2.8
CaO	0.5	1.2	0.8	1.8	1.4	1.6	1.7	1.9	1.5	1.9	1.7	1.8	1.9	1.2	1.2	1.3	1.0
Na <sub>2</sub> O	0.08	0.09	0.14	0.12	0.06	0.04	0.04	0.03	0.05	0.04	0.03	0.04	0.03	0.01	0.03	0.03	0.04
K <sub>2</sub> O	7.98	7.51	7.38	7.14	3.97	3.71	3.30	3.04	2.90	2.81	2.72	2.67	2.39	4.87	4.13	4.48	5.73
H <sub>2</sub> O (>140°C)	5.1	5.3	5.1	5.2	6.0	4.4	6.2	5.1	4.8	5.3	5.4	5.2	4.9	4.7	4.7	4.7	4.7
H <sub>2</sub> O (<140°C)	2.3	2.2	2.5	3.0	6.2	7.6	6.3	9.0	7.7	8.3	8.3	8.7	9.3	6.2	6.7	6.6	4.4
TiO <sub>2</sub>	0.34	0.54 <sup>1</sup>	0.39	1.32 <sup>1</sup>	0.28	0.29	0.14	0.18	0.11	0.14	0.12	0.13	0.12	0.28	0.79 <sup>1</sup>	0.17	2.54 <sup>1</sup>
MnO	0.07	0.18	0.05	0.03	0.02	0.02	0.02	0.02	0.01	0.01	0.02	0.02	0.02	0.01	0.02	0.02	0.0
CO <sub>2</sub>		0.50		0.14													
Total	99.4	99.4	98.0	99.6	99.1	99.5	98.4	99.0	99.9	100.2	98.7	98.2	98.7	98.8	99.5	98.9	98.2
CEC (meq/ 100 g)	15	nd	18	18	55	62	78	80	73	78	76	88	91	55	63	68	37
Sr (ppm)	31	26	47	82	75	83	103	141	139	181	182	204	232	223	314	330	220
Rb (ppm)	193	202	173	159	113	114	106	105	90	98	94	93	80	134	121	130	138
K:Sr	2135	2396	1304	723	438	371	266	179	173	129	124	109	85	181	109	113	216
K:Rb	343	308	354	373	291	270	258	240	268	238	240	239	248	301	283	286	345

<sup>1</sup> X-ray powder diffraction indicates the presence of antase.

Ordovician C-beds. The B-bed could not be sampled in the core because of core loss. Instead, this bed was sampled at Stora Mossen in an abandoned mine. In 1955, it was still possible to reach a fresh wall of the upper part of the B-bed, the lower part being below water. Nine samples were collected, B31–B39, from the top to slightly below the middle of the bed. For a complete section of the B-bed, drilling was carried out at Stora Mossen (by the Nuclear Safety Company, KBS). Only a preliminary study has been made of this material (Brusewitz, 1984).

#### Sample preparation

Twenty grams of each sample was dispersed in distilled water by gentle crushing and ultrasonic vibration. The suspensions were centrifuged to obtain the  $<1\text{-}\mu\text{m}$  fraction. No chemicals were used for dispersion, and no extractions were made in order to keep the samples in their natural state as much as possible. The collected suspensions were dried on stainless steel trays. Finally, the dried material was homogenized by gentle grinding in an agate mortar. Inasmuch as no chemicals were used, dispersion was not complete, and the  $>1\text{-}\mu\text{m}$  fractions consisted chiefly of aggregates of I/S particles.

#### Chemical analysis

Major elements were determined on the  $<1\text{-}\mu\text{m}$  fractions at the Geochemical Division of the Geological Survey of Sweden. Samples were fused in lithium borate to which cobalt and beryllium were added as reference elements. The cooled melt was ground to a fine powder, and a portion was removed for the determination of alkalis by atomic absorption, after dissolution in dilute  $\text{HNO}_3$ . Most of the powder was mixed with paper pulp and transported by a moving tape into the light arc of a direct-reading emission spectrograph (Hilger, Jumbo Model). The signals from the samples were compared to those from a set of synthetic standards. The data were evaluated by a computer program that contained corrections for overlapping and interelement interferences and reported as wt. % oxides. International standards were run concurrently to check the equipment. A summary of the method is given by Danielsson (1968). Si and Al were also analyzed by spectrophotometric methods (Shapiro and Brannock, 1956). Potassium was analyzed in connection with K-Ar age determination by the method of Cooper (1963), but using specpure  $\text{Cs}_2\text{SO}_4$  as buffering agent. The precision of the  $\text{K}_2\text{O}$  determinations was  $\pm 1.3\%$ . Ferrous iron,  $\text{CO}_2$ , water, and moisture were determined by classical methods. The precision of the reported values (except for  $\text{K}_2\text{O}$ ) has been estimated to be  $\pm 2$  relative percent. Sr and Rb were analyzed by X-ray fluorescence, with an estimated precision of  $\pm 5$  ppm. The results are listed in Table 2.

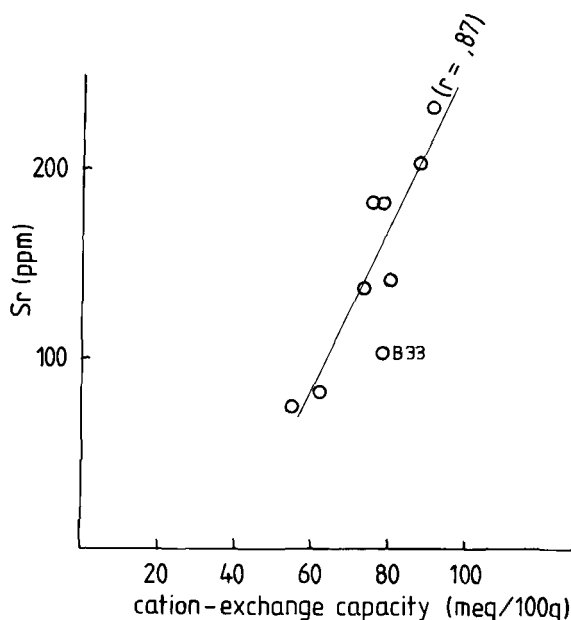


Figure 2. Plot of Sr (ppm) vs. cation-exchange capacity (CEC) (meq/100 g). Kinnekulle B-bed samples,  $<1\text{-}\mu\text{m}$  fractions.

#### Cation-exchange capacity (CEC)

The  $<1\text{-}\mu\text{m}$  fractions were treated with a 0.5 M  $\text{SrCl}_2$  solution to remove natural cations from exchangeable positions. The procedure was repeated three times; in one treatment the samples were left overnight. Excess  $\text{SrCl}_2$  was removed by repeated washings, first with distilled water, then with 1:1 water:ethanol. The air-dried powder was analyzed for Sr by X-ray fluorescence. Standards were prepared from Sr-free clay by the addition of  $\text{SrCO}_3$ . The precision is  $\pm 2$  meq/100 g. The CEC values are listed in Table 2.

#### X-ray powder diffraction (XRD)

Before drying the suspensions of the  $<1\text{-}\mu\text{m}$  fractions, a portion was removed for oriented XRD mounts. These were prepared by the suction and transfer technique of Drever (1973) after being collected by the filter technique of Brusewitz (1982). The thickness of the clay was typically  $10\text{ mg/cm}^2$ . The mounts were examined air dried as well as after ethylene glycol solvation. The treatment in an ethylene glycol atmosphere lasted for several days at  $60^\circ\text{C}$ . XRD curves were also made of randomly oriented mounts, prepared by side-ward-packing technique (Byström-Asklund, 1966). All XRD work used a Philips instrument equipped with the wide-range goniometer (PW 1050), and  $\text{CuK}\alpha$  radiation, monochromatized by a graphite crystal. A  $1^\circ$ -divergence slit, a goniometer speed of  $1^\circ/2\theta/\text{min}$ , and a paper speed of  $10\text{ mm/min}$  were used. Most of the samples were also run after treatment with warm HCl

Table 3. Structural formulae per  $O_{10}(OH)_2$  and smectite layers (%) in I/S.<sup>1</sup>

	Sample							
	K6	K13	K15	K17	B31	B32	B33	B34
<b>Tetrahedral</b>								
Si	3.38	3.41	3.34	3.45	3.67	3.64	3.70	3.72
Al	0.62	0.59	0.66	0.55	0.33	0.36	0.30	0.28
<b>Octahedral</b>								
Al	1.58	1.57	1.66	1.60	1.49	1.44	1.43	1.44
Fe <sup>3+</sup>	0.18	0.13	0.13	0.13	0.09	0.09	0.10	0.12
Fe <sup>2+</sup>	0.06	0.06	0.04	0.05	0.04	0.04	0.05	0.04
Mg	0.25	0.31	0.23	0.27	0.42	0.44	0.42	0.44
Sum	2.07	2.07	2.06	2.05	2.04	2.06	2.01	2.03
Charge	-0.10	-0.16	-0.13	-0.17	-0.34	-0.30	-0.44	-0.39
<b>Total layer charge</b>								
	-0.72	-0.75	-0.79	-0.72	-0.67	-0.66	-0.74	-0.67
<b>Interlayer</b>								
K <sub>fix</sub>	0.70	0.67	0.66	0.64	0.38	0.36	0.32	0.29
M <sup>+</sup> = sum exchangeables	0.06	0.06	0.07	0.08	0.27	0.28	0.39	0.37
Charge	0.76	0.73	0.73	0.72	0.65	0.64	0.71	0.66
<b>Smectite (%)</b>								
XRD <sup>1</sup>	8	10	10	12	35	38	41	44
Type of ordering	R=3	R=3	R=3	R=3	R=0/R=1	R=0/R=1	R=0	R=0
<b>Smectite (%) from K<sub>fix</sub>/K<sub>fix/max</sub><sup>2</sup></b>								
	4	8	10	12	48	51	56	60
<b>Corrected for</b>								
Quartz (%)					5	5	5	2
Kaolinite (%)					2	2	2	2

<sup>1</sup> % smectite layers has been derived from XRD data of Środoń (1980, 1984) and from  $K_{fix}/K_{fix/max}$ , where  $K_{fix/max} = 0.73$ .

<sup>2</sup> See text for meaning of  $K_{fix}$  and  $K_{fix/max}$ .

to differentiate between kaolinite and possible chlorite. XRD curves are shown in Figure 6.

## RESULTS

### Zonation of the B-bed

The analyses (see Table 2) show a clear zonation of the B-bed. From the center upwards,  $K_2O$  increases

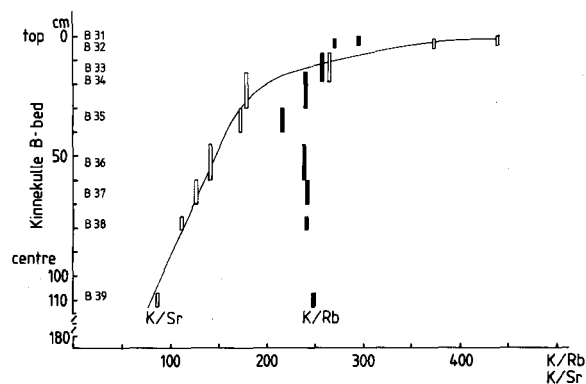


Figure 3. Plot of K:Sr and K:Rb ratios in relation to depth in B-bed. Scale at left shows distance from upper contact in centimeters. Open bars = K:Sr, filled bars = K:Rb ratios. Length of bar indicates sampling interval.

and CEC decreases.  $K_2O$  vs. CEC shows a linear regression having a correlation coefficient of  $r = -0.91$ . With the increase in K and the formation of illite layers, exchangeable ions, chiefly Ca, apparently moved out of the structure and most likely precipitated as carbonate. Thin selvages of calcite are irregularly distributed in the bentonites and may have formed from such expelled Ca. These selvages were avoided when the samples were collected. Sr appears to have been exclusively bound in smectite layers. Assuming that CEC is a measure of the smectite proportion of I/S (Figure 2), as illite layers formed, Sr was also expelled. It most likely precipitated with Ca and is no longer part of the bulk bentonite.

The zonation of the B-bed is also obvious from the K:Sr ratios, representative of the I/S ratio (Figure 3). From the center upwards, K:Sr gradually increases from 100 to 200. At about 20 cm from the top of the bed, the ratio changes abruptly to  $>400$ , indicating special boundary conditions.

The K:Rb ratio is also shown in Figure 3. Both elements, associated only with illite layers, have a constant ratio from the center upwards to about 20 cm from the top, at which point K:Rb increases but not as abruptly as K:Sr. Samples B33–B39 show a mean

Table 3. Continued.

Sample								
B35	B36	B37	B38	B39	K71	K72	K74	K78
3.71	3.67	3.71	3.72	3.75	3.67	3.70	3.65	3.59
0.29	0.33	0.29	0.28	0.25	0.33	0.30	0.35	0.41
1.40	1.40	1.42	1.42	1.42	1.52	1.53	1.49	1.59
0.11	0.12	0.12	0.12	0.12	0.10	0.11	0.13	0.09
0.06	0.07	0.06	0.06	0.05	0.04	0.05	0.05	0.05
0.41	0.48	0.45	0.42	0.44	0.36	0.33	0.35	0.30
2.02	2.07	2.03	2.02	2.03	2.02	2.02	2.02	2.03
-0.41	-0.34	-0.34	-0.42	-0.40	-0.34	-0.32	-0.34	-0.26
-0.70	-0.67	-0.71	-0.70	-0.65	-0.67	-0.62	-0.69	-0.67
0.30	0.27	0.28	0.26	0.23	0.43	0.37	0.40	0.52
0.40	0.41	0.40	0.43	0.43	0.23	0.26	0.29	0.16
0.70	0.68	0.68	0.69	0.66	0.66	0.63	0.69	0.68
46	46	49	51	54	30	35	30	25
R=0	R=0	R=0	R=0	R=0	R=0/R=1	R=0/R=1	R=0/R=1	R=1
59	63	62	64	68	41	49	45	29
8	5	5	3	2				
4	5	2	3	2				

K:Rb value of  $247 \pm 11$ , which is similar to earlier reported values of 240 for post-Precambrian illitic and mixed-layer clays (Horstman, 1957) and 252 for Precambrian illites, rich in the *1Md* polytype, reported by Reynolds (1963). At the top of the B-bed, K:Rb is nearly 300, similar to values found for the thicker C-beds. One thin C-bed, sample K78, and the Silurian samples show values as great as 373 (Table 2).

Structural formulae were calculated from the chemical analyses in Table 2 on the basis of  $O_{10}(OH)_2$  (Table 3). The B-bed samples were corrected for quartz and kaolinite as estimated from XRD. CEC values were similarly corrected. HCl-extractions were used to check any change in the 7-Å reflection due, perhaps, to the dissolution of chlorite. The Silurian samples, which contained minor amounts of impurities (chiefly chlorite), were not corrected, because estimation of the amount of impurities was difficult. For sample K17 the CaO value was not used and exchangeable ions were based on CEC only. Ti was not included in the formulae because XRD showed anatase to be present in many of the samples.  $M^+/O_{10}(OH)_2$  was calculated from the CEC values;  $M^+$  is the sum of exchangeable ions (chiefly  $Ca^{2+}$  and  $Mg^{2+}$ ) as equivalents (Byström, 1956). In the calculations all CaO and  $Na_2O$  (the latter

being present in subordinate amounts) were regarded as exchangeable, and all  $K_2O$  as fixed. Exchangeable  $Mg^{2+}$  was obtained by subtracting the sum of Ca and Na equivalents from  $M^+$ , and the remaining part was assigned to the octahedral sheet (Foster, 1951).

The structural formulae show Silurian samples to have high octahedral occupancy and unbalanced charge, because no corrections were made for impurities. The formulae do, however, show the highly illitic character of these samples. Two samples in the B-bed series, B32 and B36, also show high octahedral occupancy, possibly due to poorly estimated impurities, but the trend of the series is still clear.

Figure 4 is a plot of Si vs. fixed K per  $O_{10}(OH)_2$  (see Table 3). The line extrapolated to  $K_{fix} = 0$  intersects the Si-axis at 3.95. This value suggests that the original smectite was montmorillonitic ( $Si_4$ ) rather than beidellitic ( $Si_{4-x}Al_x$ ) and that Al substitution in this sheet took place during the formation of the illite layers. Figure 5 is a plot of  $M^+$  (exchangeable cations) vs.  $K_{fix}$  per  $O_{10}(OH)_2$ . Extrapolation of the line to  $M^+ = 0$  gives a  $K_{fix/max} = 0.73$ , a value similar to that obtained by Inoue and Utada (1983) in a plot of five different I/S series. The  $K_{fix/max}$  value obtained in the present study was used to calculate the percentage of illite layers

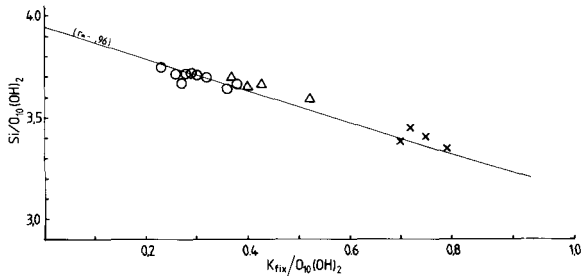


Figure 4. Plot of Si vs.  $K_{\text{fix}}$  per  $\text{O}_{10}(\text{OH})_2$ ; data from Table 3. (O) = B-beds, ( $\Delta$ ) = C-beds, ( $\times$ ) = Silurian bentonites.

(from  $K_{\text{fix}}/0.73$ ). Postulating only illite and smectite layers, the result given in Table 3 is expressed as % smectite layers. These data imply a constant  $K_{\text{fix}}$  for all illite layers, a conclusion questioned by Środoń *et al.* (1986) and which will be discussed below.

Extrapolation of the line in Figure 5 in the other direction to  $K_{\text{fix}} = 0$  gives  $M^+_{\text{max}} = 0.62$ , a high value compared to 0.4, the average charge of the "pure" smectite layer (Weaver and Pollard, 1973). These authors, however, also stated that values as large as 0.60–0.65 are legitimate maximum values. In addition the relation of total layer charge to  $K_{\text{fix}}$  does not correspond to published observations which show that layer charge decreases with decreasing  $K_{\text{fix}}$  (Eslinger *et al.*, 1979). For the Kinnekulle Ordovician samples, the total layer charge is constant at  $0.68 \pm 0.03$ , although  $K_{\text{fix}}$  changes from 0.23 to 0.52.

Comparisons of  $M^+_{\text{max}}$  and  $K_{\text{fix}/\text{max}}$  with those of published I/S series (Table 4) show the  $M^+_{\text{max}}$  values, except for the Kinnekulle series, to have fairly concordant values of about 0.4. The  $K_{\text{fix}/\text{max}}$  shows a greater spread, being highest (0.90) for the Polish clays. Thus, these discrepancies probably do not reflect different I/S compositions; more likely, they result from different sample pretreatments, in particular, citrate extraction (Mehra and Jackson, 1960).

#### X-ray powder diffraction

XRD curves of randomly oriented samples show only  $hk$  reflections at about 4.48, 2.57, and 1.50 Å as distinct peaks. Even the most illitic sample (sample K6) shows no sharp  $hkl$  reflections, suggesting thin crystallites and poor crystallinity. The 060 peak at 1.50 Å suggests a dioctahedral structure.

The percentages of smectite layers in I/S estimated from the XRD patterns shown in Figure 6 by using the methods of Środoń (1980, 1984) are given in Table 3. Within the B-bed samples, the position of the 17-Å reflection is essentially constant, although  $K_{\text{fix}}/\text{O}_{10}(\text{OH})_2$  ranges from 0.23 to 0.38. Samples B31 and B32, from the upper contact, display what appears to be a superlattice peak at 30 Å before the 17-Å peak disappears. Concerning the transition from random ( $R=0$ ) to reg-

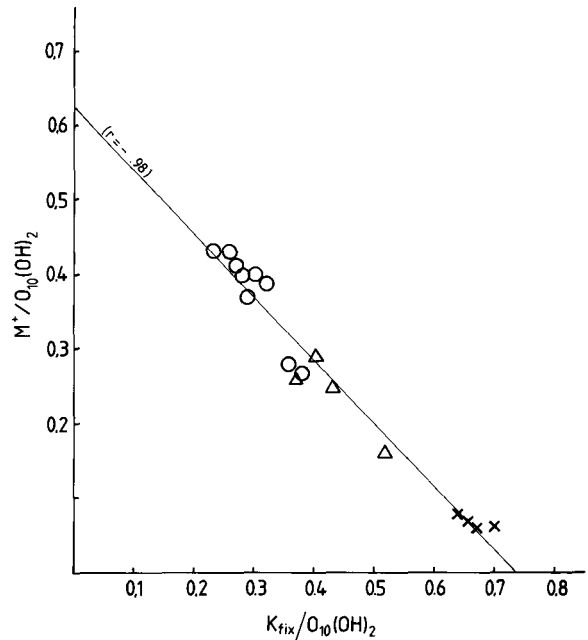


Figure 5. Plot of  $M^+$  vs.  $K_{\text{fix}}$  per  $\text{O}_{10}(\text{OH})_2$ , data from Table 3. Extrapolation to  $M^+ = 0$  gives  $K_{\text{fix}/\text{max}} = 0.73$ . Symbols as in Figure 4.

ular ( $R=1$ ) alternation of layers, a zone seems to be present in which at the same  $K_{\text{fix}}$  both types of ordering exist; e.g., the I/S ordering of sample B31 is nearly random and that of samples K72 and K74 is ordered. A higher Al:Mg ratio in the octahedral sheet of the more ordered samples may explain these structural differences.

As the proportion of illite layers increases (i.e., an increase in  $K_{\text{fix}}$ ), no obvious change was observed in the position of the 17-Å peak of B-bed samples (see Figure 7), only the shape of the peak changes (see Figure 6a). As the number of illite layers in the I/S increases, the peak becomes weaker and broader, and the background on the low-angle side of the peak increases. This saddle-to-peak ratio has been used to estimate I/S proportions (Weir *et al.*, 1975; Eslinger and Savin, 1976; Hoffman, 1976). Because of the many parameters involved (Środoń, 1981) the method cannot be generally applied; however, in the present study of samples that had been uniformly treated with regard to sample preparation, chemical analysis, and XRD examination, a close relation between peak shape and chemistry is apparent. In Figure 8 saddle: peak intensity ratios are plotted against  $K_{\text{fix}}/\text{O}_{10}(\text{OH})_2$ . Heights of saddle ( $h_1$ ) and peak ( $h_2$ ) were measured from the lowest point of the background near  $8^\circ 2\theta$ . For ordered samples, the intensity of the superlattice peak at about  $3^\circ 2\theta$  was taken as  $h_1$ . B-bed samples having random ordering ( $R=0$ ) plot on a straight line ( $r = -0.94$ ). Samples having  $R > 0$  ordering are also linearly related ( $r = -0.98$ ),

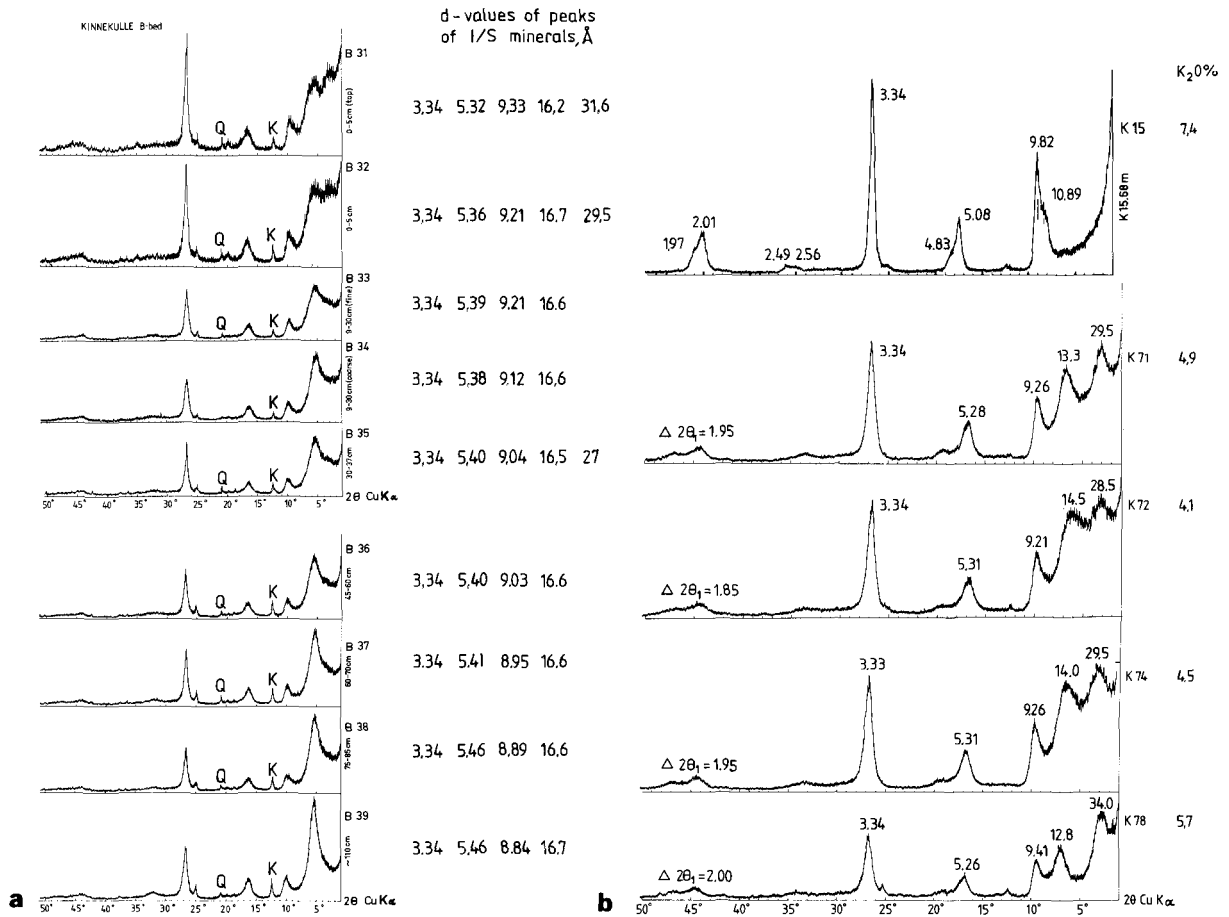


Figure 6. (a) X-ray powder diffraction curves of Kinnekulle B-bed samples, <1- $\mu$ m fraction; ethylene-glycol solvated, oriented mounts. Peaks of kaolinite (K) and quartz (Q) are marked on curves. To the right of the curves, d-values of peaks from I/S minerals are listed. CuK $\alpha$  radiation. (b) X-ray powder diffraction curves of Silurian bentonite, K15, and C-bed samples (K71, K72, K74, and K78), <1- $\mu$ m fraction; ethylene-glycol solvated, oriented mounts. d-values in Å are marked on the curves.  $\Delta 2\theta_1$  is measured according to Środoń (1980) from curves of higher sensitivity; CuK $\alpha$  radiation.

but the line has a slightly different slope from that of the R=0 samples.

The difference between the d-values of two variable peaks ( $\Delta = l_1 - l_2$ ) is related to K<sub>2</sub>O content (Figure 9),  $l_1$  and  $l_2$  being the peaks that range from 5.3° to 8.1° and 8.7° to 10.0°2 $\theta$ , respectively. In a mineral assemblage containing no other K minerals or containing K minerals in only subordinate amounts (e.g., assemblages of quartz, chlorite, and kaolinite), the amount of I/S present can be estimated from the K<sub>2</sub>O<sub>total</sub>/K<sub>2</sub>O<sub>I/S</sub> ratio. The method is not precise, however, for smectite-rich I/S and random interstratifications.

## DISCUSSION

### Estimation of proportion of smectite layers in I/S

The proportion of smectite layers in I/S (Table 3) was estimated in two ways: (1) from XRD by the methods of Środoń (1980, 1984), and (2) from K<sub>fix</sub> in the

structural formulae. The XRD-derived values were lower. A comparison between the methods was made by plotting the percentage of smectite layers vs. CEC and extrapolating to 100% smectite layers. The XRD method gave a CEC value of 194 meq/100 g; and the K<sub>fix</sub> method, a value of 147 meq/100 g. The lower value is more in accord with the CEC of pure smectites.

### Conversion of smectite to illite

Effects from the diabase intrusion could have masked previous diagenetic reactions in the Kinnekulle bentonites. A time span of 150 m.y. exists between the volcanic ash fall at about 450 Ma and the intrusion of the diabase at about 300 Ma. The volcanic ash was deposited in a marine environment in the Iapetus Ocean. Other studies on K-bentonites, e.g., Środoń (1976) and Huff and Türkmenöglü (1981), considered that initially smectite formed from the volcanic glass,



Table 4. Comparison of  $M^+_{max}$  and  $K_{fix/max}$  per  $O_{10}(OH)_2$  between different series of illite/smectites (see source), plotted as in Figure 5. Correlation coefficients,  $r$ , for the linear regressions are shown; for  $M^+_{max}$  and  $K_{fix/max}$  see text.

Bentonites	$M^+_{max}$	$K_{fix/max}$	Corr. coeff. ( $r$ )	No. of samples	Source
Silurian and Ordovician Kinnekulle, Sweden	0.62	0.73	-.98	17	This paper
Silurian Welsh Borderland United Kingdom	0.45	0.81	-.98	10	Środoń <i>et al.</i> (1986)
Carboniferous Silesia, Poland (Sr-exchanged clays) <sup>1</sup>	0.36	0.90	-.96	12	Środoń <i>et al.</i> (1986)
Cretaceous Montana, U.S.A.	0.41	0.65	-.99	17	Eslinger <i>et al.</i> (1979) also in Środoń <i>et al.</i> (1986)
Miocene Waga-Omo-so, Japan	0.46	0.74	-.98	12	Inoue <i>et al.</i> (1978)

<sup>1</sup> The Na-exchanged samples showed a great spread and did not extrapolate in a meaningful way.

and that at a later stage illite formed when K became available from an outside source. The same process is believed to have occurred for the Kinnekulle bentonites, a montmorillonite-type smectite first being formed as suggested from Figure 4. The higher K:Rb ratios at contacts and in the thin beds suggest that these areas were saturated with formation brines having a high K:Rb ratio (Mason, 1966) for longer periods than the centers of the thicker beds. The process may have been diffusion controlled, as suggested by Altaner *et al.* (1984).

An estimate of the temperatures that prevailed at Kinnekulle can be obtained from conodont colors (Bergström, 1980). Conodonts collected near the Silurian bentonites show a color alteration index (CAI) of 6, indicating temperatures  $>300^\circ\text{C}$ , no upper temperature being given. The Silurian bentonites show conversion of smectite nearly all the way to illite (i.e.,  $<10\%$  smectite layers).

Conodonts from the Ordovician strata indicate lower temperatures. The Skagen limestone, sampled at Stora Mossen above the B-bed gave CAI values of 4; those from the Dalby Limestone below the B-bed gave CAI values of 3. These values correspond to temperatures of  $190^\circ\text{--}300^\circ$  and  $110^\circ\text{--}200^\circ\text{C}$ , respectively. Still deeper in the strata (and further from the diabase) in the Gulhøgen Formation (Figure 1) a CAI of 1.5 was calculated, equivalent to temperatures of  $50^\circ\text{--}90^\circ\text{C}$ .

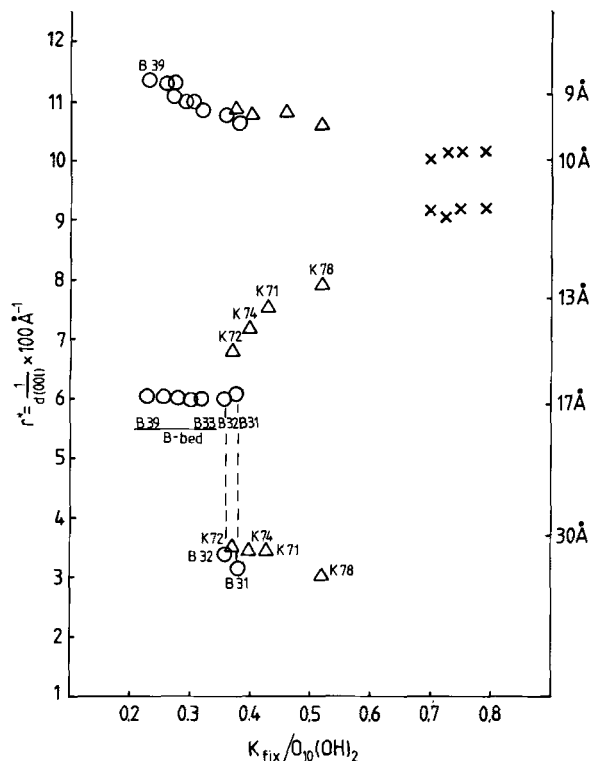


Figure 7. Plot of X-ray powder diffraction positions in reciprocal units ( $r^* = \frac{1}{d} 100 \text{ \AA}^{-1}$ ) vs.  $K_{fix}/O_{10}(OH)_2$ ; symbols as in Figure 4.

Most likely, the temperatures indicated are on the high side inasmuch as the period of heating must have been shorter than that of the CAI reference scale (Harris, 1979). The relative decrease in temperature downwards in the strata shows that burial diagenesis of the type described by Perry and Hower (1970) was not active in the Kinnekulle bentonites or that it has been overprinted by the heating effect of the diabase. These conclusions appear to be true also for many other K-bentonites (Parachoniak and Środoń, 1973; Snäll, 1977; Schultz, 1978; Pevear *et al.*, 1980; Huff and Türkmenöglü, 1981; Altaner *et al.*, 1984).

The Ordovician bentonites at Kinnekulle are located within a single 12-m-thick sedimentary sequence; temperature differences within this narrow interval might be expected to have been minor; however, based on CAI values, the temperature decreased downward, meaning that C-beds, which have a high proportion of illite layers in I/S, reacted at a lower temperature than the more smectitic B-bed above. Thus, factors other than temperature were probably important in the smectite-to-illite reaction.

To systematize different stages of the smectite-illite series, Inoue and Utada (1983, Figures 5 and 9) used the migration of XRD peaks after the model of Wa-

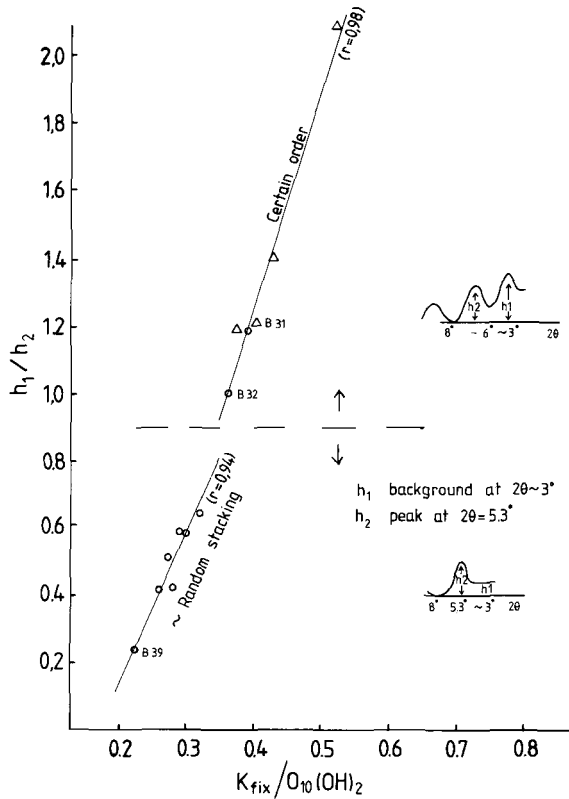


Figure 8. Plot of saddle-to-peak relation,  $h_1/h_2$ , vs.  $K_{fix}/O_{10}(OH)_2$ . Small sketches in right-hand side of figure indicate how  $h_1$  and  $h_2$  were measured; symbols as in Figure 4.

tanabe (1981). In Figure 10 their diagram is modified to include Kinnekulle samples. These samples fill the gap in the Inoue and Utada (1983) plot. Inoue and Utada (1983) indicated a "diagenetic" field and arrows showing the hydrothermal trend, the latter along the  $g = 1$  line ( $R=1$  of Reynolds, 1980). The B-samples all fall in the diagenetic field, whereas two of the C-bed samples are in the diagenetic field and two are close to the  $g = 1$  line. Nothing suggests that the reaction mechanism was different for the C-bed samples. The extrapolated path of the  $g = 1$  line, proposed for hydrothermally reacted samples, apparently suits samples with a different chemistry, such as the Roseki samples which have Na in the interlayer position instead of K. Thus, crystal-chemical criteria rather than reaction mechanisms decide where samples will fall in the scheme.

### Zonation

It is obvious that the thickness of a bentonite bed had a major influence on the degree of illite formation, as has been found for "whole rock" samples from Kinnekulle studied by Velde and Brusewitz (1982). Recently, Altaner *et al.* (1984) described beds similar to, but younger than, those at Kinnekulle, in K-bentonites

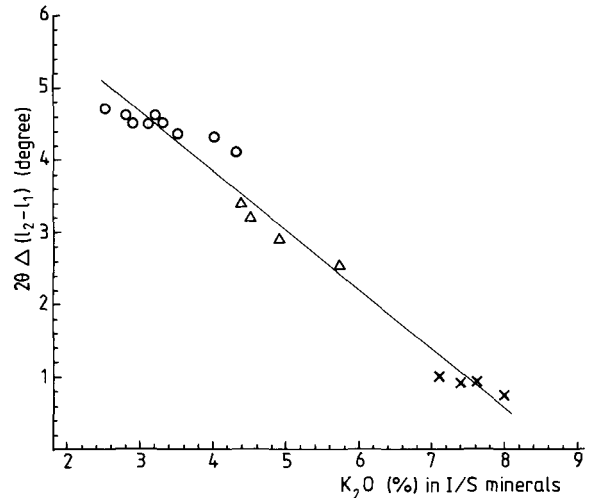


Figure 9. Plot of  $\Delta(l_2 - l_1)$  vs.  $K_2O$  (%) in I/S minerals;  $l_1$  = peak varying between  $5.3^\circ$ – $8.1^\circ 2\theta$ , and  $l_2$  = peak varying between  $8.7^\circ$ – $10.0^\circ 2\theta$ ,  $CuK\alpha$  radiation.  $K_2O$  (%) from Table 2 and corrected for impurities as shown in Table 3. Curve for a rough estimate of  $K_2O$  in illite/smectite (I/S) minerals. If  $K_2O$  in the total sample is known, the amount of I/S can be obtained, provided only minor quantities of other potassium-bearing minerals are present; symbols as in Figure 4.

from the disturbed belt, Montana. One 2.5-m-thick bed showed clear zonation, with greater proportions of illite layers in I/S at the contacts. Thinner beds, if  $>90$  cm thick, also showed zonation. I/S minerals in the thinner beds contained the same proportion of illite and smectite layers as those at the contact of the thick bed. At Kinnekulle, a distinct zonation is apparent from the center of the B-bed towards its upper boundary; I/S at the boundary contained about 20% less smectite layers than I/S at the center of the bed. Preliminary data on the lower half of the bed failed to show such a zonation downwards (Brusewitz, 1984). Instead, according to XRD data, the smectite proportion in the I/S was constant at about 50% smectite layers.

Variations in geologic setting of the two areas described above may explain why the reactions differed. The Kinnekulle bentonite is flat-lying, and the lower contact shows silicification, probably a side effect of the alteration of volcanic glass to smectite, which slowed or hindered diffusion. The Montana bed, on the other hand, is tilted because of thrusting (Mudge, 1972; S. J. Altaner, Department of Geology, University of Illinois, Urbana, Illinois, personal communication, 1985), which made diffusion from both contacts equally possible. K/Ar age determinations of the Montana beds gave ages of 54–56 Ma at the contacts and ages 3–4 m.y. younger at the center. Similar K/Ar age determinations of the Kinnekulle B-bed gave 336 Ma for the upper contact and about 300 Ma for samples collected at the center, a difference of 36 m.y. within a

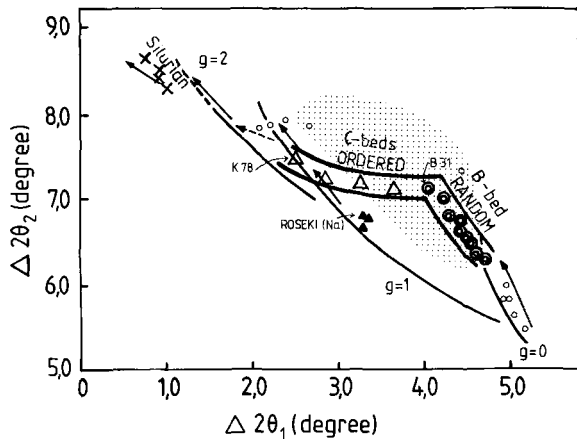


Figure 10. Plot of  $\Delta 2\theta_2$  vs.  $\Delta 2\theta_1$ , modified after Inoue and Utada (1983, Figures 5 and 9);  $\Delta 2\theta_1 = l_2 - l_1$  and  $\Delta 2\theta_2 = l_3 - l_2$ , where  $l_1$  is the reflection that varies between  $5.1^\circ$  and  $7.6^\circ$ ,  $l_2$  between  $8.9^\circ$  and  $10.2^\circ$ , and  $l_3$  between  $16.1^\circ$  and  $17.5^\circ 2\theta$ ,  $\text{CuK}\alpha$  radiation.  $g = 0$ ,  $g = 1$ , and  $g = 2$  correspond to  $R=0$ ,  $R=1$ , and  $R=2$  of Reynolds (1980). Kinnekulle samples are added. The random B-bed samples ( $\odot$ ) continue the  $g = 0$  line beyond the marked extrapolation (from the original figure). The ordered C-bed samples ( $\Delta$ ) link up with the random samples but break into a new direction towards the  $g = 1$  line, the most ordered sample, K78, falling on this line. The B-bed sample, B31, from the top boundary has an intermediate position, belonging to both series. The Roseki samples ( $\blacktriangle$ ) with Na instead of K in the illite interlayer fall in a different field. The shaded area corresponds to the diagenetic field in the original figure. Arrows show hydrothermal trends. The Silurian samples ( $\times$ ) plot in the same region as the illitic samples of the paper cited.

thickness of only about 1 m, 10 times greater than for a similar distance in the Montana bed.

The availability of K in the surrounding rocks (shale vs. carbonate) is important to the smectite-to-illite reaction (Altaner *et al.*, 1984). Nadeau and Reynolds (1981) found that the percentage of illite layers in I/S was lower in calcareous environments than in non-calcareous environments. These findings are supported by hydrothermal experiments which show that the ratio of  $\text{K}^+$  to  $\text{Ca}^{2+}$  to  $\text{Mg}^{2+}$  is particularly important, the divalent ions inhibiting the smectite-to-illite reaction (Eberl, 1978; Roberson and Lahann, 1981; Inoue, 1983). A plausible mechanism for the smectite-to-illite reaction can be deduced from the experiments of Lahann and Roberson (1980) (time and temperature necessarily being different), in which a mildly alkaline bicarbonate buffer ( $\text{pH} = 9$ ) was used to study the dissolution of silica from montmorillonite—a reaction that is strongly dependent on the ratios of  $\text{K}^+:\text{Ca}^{2+}$ ,  $\text{K}^+:\text{Mg}^{2+}$ , and  $\text{K}^+:\text{Na}^+$ . A low ratio of mono- to divalent ions retards the reaction. A mildly alkaline environment may have prevailed at Kinnekulle in which silica, alkalis, and most of the other reacting elements, such as Al, Ca, Sr, and Mg, probably entered solution as

ions or ion complexes. As the proportion of smectite layers in I/S decreased, Sr was removed from the system, most likely precipitated with Ca as carbonate. Al was apparently abundant, but did not limit the smectite-to-illite reaction, as evidenced by the presence of kaolinite.

## CONCLUSIONS

The Kinnekulle bentonites contain I/S ranging from random ( $R=0$ ) and containing 50–60% smectite layers to those having greater order ( $R=1$ ,  $R=3$ ) and containing as much as 90% illite layers. Data derived from chemical analyses do not support earlier data based on XRD determinations. Thus, the charge of  $M^+$ , extrapolated to  $K_{\text{fix}} = 0$ , is  $0.62/\text{O}_{10}(\text{OH})_2$ , which is high compared with reported value for montmorillonite of about 0.3–0.4 (Weaver and Pollard, 1973; Eslinger *et al.*, 1979; Środoń *et al.*, 1986). The nearly constant value of total layer charge ( $0.68 \pm 0.03$ ) for a variation of  $K_{\text{fix}}$  of 0.23 to 0.52 per  $\text{O}_{10}(\text{OH})_2$  has not been previously documented. Differences in the pretreatment of the samples or the analytical techniques may have influenced the results.

All the  $R=0$  I/S samples were collected from the 2-m-thick B-bed, which showed an increasing percentage of illite layers towards the upper contact. Preliminary values from the lower half of the bed did not show the same systematic change of K content and proportion of illite layers in I/S that was found by Altaner *et al.* (1984), probably due to the difference in the two geologic environments. The age difference between the top and the center of the bed (36 m.y.) is not clearly understood. Illite layers may have started to form at about 336 Ma, and then, during the intrusion of the diabase at about 300 Ma, the reaction went to completion with the formation of the K-bentonite that is present today.

The thinner C-beds show a higher regularity in I/S ordering than the B-bed; in the former beds a zonation can be seen too, in which higher proportions of smectite layers in I/S are found in the middle of a given bed. The thin Silurian beds nearest the diabase have reacted to nearly pure illite.

The extent to which the conversion of smectite-to-illite took place appears to have been partly dependent on temperature, mainly provided by the diabase intrusive. If the temperature was the same for all beds, diffusion and chemical environment must have governed the extent of the reaction. The removal of Ca and Mg was apparently important, as was a source of K, both of which led to faster reaction (more complete conversion) in the thin beds than in thick beds at a given temperature. Reaction was slowest at the center of the thick beds.

## ACKNOWLEDGMENTS

I thank many of the staff of the Geological Survey of Sweden for various assistance during this work, in particular, S. Snäll and G. Nordmark. I am grateful to Bruce Velde and to T. Alexandersson (Uppsala University) for comments and constructive criticism. I also acknowledge contributions from the Swedish Scientific Research Council.

## REFERENCES

- Altaner, S. P., Hower, J., Whitney, G., and Aronson, J. L. (1984) Model for K-bentonite formation: evidence from zoned K-bentonites in the disturbed belt, Montana: *Geology* **12**, 412–415.
- Bergström, S. M. (1980) Conodonts as paleotemperature tools in Ordovician rocks of the Caledonides and adjacent areas in Scandinavia and the British Isles: *Geol. Fören. Stockholm Förh.* **102**, 377–392.
- Brusewitz, A. M. (1982) A filtering device for oriented XRD mounts: *Clay Miner.* **17**, 263–264.
- Brusewitz, A. M. (1984) Preliminary report on potassium bentonites in Sweden. A study of illite-smectite minerals: in *Smectite Alteration*, D. M. Andersson, compiler, Swedish Nuclear Fuel and Waste Management Co. Tech. Rept. **84-11**, 105–121.
- Byström, A. M. (1954) 'Mixed layer' minerals from Ordovician bentonite beds at Kinnekulle, Sweden: *Nature* **173**, 783.
- Byström, A. M. (1956) Mineralogy of the Ordovician bentonite beds at Kinnekulle, Sweden: *Sver. Geol. Unders. Serie C, No. 540*, 62 pp.
- Byström-Asklund, A. M. (1966) Sample cups and a technique for sideward packing of X-ray diffractometer specimens: *Amer. Mineral.* **51**, 1234–1237.
- Byström-Asklund, A. M., Baadsgaard, H., and Folinsbee, R. E. (1961) K/Ar age of biotite, sanidine and illite from Middle Ordovician bentonites at Kinnekulle, Sweden: *Geol. Fören. Stockholm Förh.* **83**, 92–96.
- Cooper, J. A. (1963) The flame photometric determination of potassium in geological materials used for potassium-argon dating: *Geochim. Cosmochim. Acta* **27**, 525–546.
- Danielsson, A. (1968) Spectrochemical analysis for geochemical purposes: in *Proc. 13th Colloquium Spectroscopium Internationale*, Neville Goodman, ed., Adam Hilger Ltd., London, 311–323.
- Drever, J. J. (1973) The preparation of oriented clay mineral specimens for X-ray diffraction of analysis by a filter membrane peel technique: *Amer. Mineral.* **58**, 553–554.
- Eberl, D. D. (1978) The reaction of montmorillonite to mixed-layer clay: the effect of interlayer alkali and alkaline cations: *Geochim. Cosmochim. Acta* **42**, 1–7.
- Eslinger, E., Highsmith, P., Albers, D., and De Mayo, B. (1979) Role of iron in the conversion of smectite to illite in bentonites in the disturbed belt, Montana: *Clays & Clay Minerals* **27**, 327–338.
- Eslinger, E. V. and Savin, S. M. (1976) Mineralogy and O<sup>18</sup>/O<sup>16</sup> ratios of fine-grained quartz and clay from site 323: in *Init. Reports on the Deep Sea Project 35*, Paula Worstell, ed., U.S. Government Printing Office, Washington, D.C., 489–496.
- Foster, M. D. (1951) The importance of exchangeable magnesium and cation-exchange capacity in the study of montmorillonitic clay: *Amer. Mineral.* **36**, 717–730.
- Harris, A. G. (1979) Conodont color alteration, an organomineral metamorphic index, and its application to Appalachian basin geology: *Soc. Econ. Paleon. Mineral., Spec. Pub.* **26**, 3–16.
- Hoffman, J. (1976) Regional metamorphism and K/Ar dating of clay minerals in Cretaceous sediments of the disturbed belt of Montana: Ph.D. thesis, Case Western Reserve University, Cleveland, Ohio, 266 pp.
- Horstman, E. L. (1957) The distribution of lithium, rubidium, and cesium in igneous and sedimentary rocks: *Geochim. Cosmochim. Acta* **12**, 1–28.
- Hower, J. and Mowatt, T. C. (1966) The mineralogy of illite and mixed-layer illite/montmorillonites: *Amer. Mineral.* **51**, 825–854.
- Huff, W. D. and Türkmenöglü, A. G. (1981) Chemical characteristics and origin of Ordovician K-bentonites along the Cincinnati arch: *Clays & Clay Minerals* **29**, 113–123.
- Inoue, A. (1983) Potassium fixation by clay minerals during hydrothermal treatment: *Clays & Clay Minerals* **31**, 81–91.
- Inoue, A., Minato, H., and Utada, M. (1978) Mineralogical properties and occurrence of illite/montmorillonite mixed-layer minerals formed from Miocene volcanic glass in Waga-Omono district: *Clay Sci.* **5**, 123–136.
- Inoue, A. and Utada, M. (1983) Further investigations of a conversion series of dioctahedral mica/smectites in the Shinzan hydrothermal alteration area, northeast Japan: *Clays & Clay Minerals* **31**, 400–412.
- Jaanusson, V. (1964) The Viruan (Middle Ordovician) of Kinnekulle and northern Billingen, Västergötland: *Bull. Geol. Inst. Univ. Uppsala* **43**, 73 pp.
- Johansson, S., Sundius, N., and Westergård, A. H. (1943) Description of the mapsheet "Lidköping": *Sver. Geol. Unders. Ser. Aa No. 182*, 197 pp. (in Swedish).
- Kunk, M. D., Sutter, J., and Bergström, S. H. (1984) <sup>40</sup>Ar-<sup>39</sup>Ar age spectrum dating of biotite and sanidine from Middle Ordovician bentonites of Sweden: a comparison with results from eastern North America: in *Abstracts with Prog., Geol. Soc. Amer.* **16**, p. 566.
- Lahann R. W. and Roberson, H. E. (1980) Dissolution of silica from montmorillonite: effect of solution chemistry: *Geochim. Cosmochim. Acta* **44**, 1937–1943.
- Mason, B. (1966) *Principles of Geochemistry*: 3rd ed., Wiley, New York, 329 pp.
- Mehra, O. P. and Jackson, M. L. (1960) Iron oxide removal from soils and clays by a dithionite-citrate system buffered with sodium bicarbonate: in *Clay and Clay Minerals, Proc. 7th Natl. Conf., Washington, D.C., 1958*, Ada Swineford, ed., Pergamon Press, New York, 317–327.
- Mudge, M. R. (1972) Pre-Quaternary rocks in the Sun River Canyon area, northwestern Montana: *U.S. Geol. Surv. Prof. Pap.* **663-A**, 142 pp.
- Nadeau, P. H. and Reynolds, R. C., Jr. (1981) Burial and contact metamorphism in the Mancos Shale: *Clays & Clay Minerals* **29**, 249–259.
- Parachoniak, W. and Środoń, J. (1973) The formation of kaolinite, montmorillonite and mixed-layer montmorillonite-illites during the alteration of Carboniferous tuff (the Upper Silesian coal basin): *Mineral. Pol.* **4**, 37–52.
- Perry, E. A. and Hower, J. (1970) Burial diagenesis in Gulf Coast pelitic sediments: *Clays & Clay Minerals* **18**, 165–178.
- Pevear, D. R., Williams, V. E., and Mustoe, G. E. (1980) Kaolinite, smectite, and K-rectorite in bentonites: relation to coal rank at Tulameen, British Columbia: *Clays & Clay Minerals* **28**, 241–254.
- Priem, H. N. A., Mulder, F. G., Boelrijk, N. A. I. M., Hebeda, E. H., Verschure, R. H., and Verdurmen, E. A. Th. (1968) Geochronological and paleomagnetic reconnaissance sur-

- vey in parts of central and southern Sweden: *Phys. Earth Planet. Interiors* **1**, 373–380.
- Reynolds, R. C., Jr. (1963) Potassium-rubidium ratios and polymorphism in illites and microclines from clay size fractions of Proterozoic carbonate rocks: *Geochim. Cosmochim. Acta* **27**, 1097–1112.
- Reynolds, R. C. (1980) Interstratified minerals: in *Crystal Structures of Clay Minerals and their X-ray Identification*, G. W. Brindley and G. Brown, eds., Mineralogical Society, London, p. 255.
- Reynolds, R. C., Jr. and Hower, J. (1970) The nature of interlayering in mixed-layer illite-montmorillonites: *Clays & Clay Minerals* **18**, 25–36.
- Roberson, H. E. and Lahann, R. W. (1981) Smectite to illite conversion rates: effects of solution chemistry: *Clays & Clay Minerals* **29**, 129–135.
- Schultz, L. G. (1978) Mixed-layer clay in the Pierre Shale and equivalent rocks, northern Great Plains region: *U.S. Geol. Surv. Prof. Pap.* **1064-A**, 28 pp.
- Shapiro, L. and Brannock, W. W. (1956) Rapid analysis of silicate rocks: *U.S. Geol. Surv. Bull.* **1036C**, 56 pp.
- Skoglund, R. (1963) Uppermost Viruan and lower Harjuan (Ordovician) stratigraphy of Västergötland, and lower Harjuan Graptolite Faunas of central Sweden: *Bull. Geol. Inst. Univ. Uppsala* **42**, 55 pp.
- Snäll, S. (1977) Silurian and Ordovician bentonites of Gotland (Sweden): *Acta Univ. Stockholm, Contrib. Geol.* **31**, 80 pp.
- Środoń, J. (1976) Mixed-layer smectites/illites in bentonites and tonsteins of Upper Silesian coal basin: *Pol. Akad. Nauk. Pr. Mineral.* **49**, 84 pp.
- Środoń, J. (1980) Precise identification of illite/smectite interstratification by X-ray powder diffraction: *Clays & Clay Minerals* **28**, 401–411.
- Środoń, J. (1981) X-ray identification of randomly interstratified illite-smectites in mixtures with discrete illite: *Clay Miner.* **16**, 297–304.
- Środoń, J. (1984) X-ray powder diffraction identification of illitic materials: *Clays & Clay Minerals* **32**, 337–349.
- Środoń, J., Morgan, D. J., Eslinger, E. V., Eberl, D. D., and Karlinger, M. R. (1986) Chemistry of illite/smectite and end-member illite: *Clays & Clay Minerals* **34**, 368–378.
- Velde, B. and Brusewitz, A. M. (1982) Metasomatic and non-metasomatic low-grade metamorphism of Ordovician meta-bentonites in Sweden: *Geochim. Cosmochim. Acta* **46**, 447–452.
- Waern, B., Thorslund, P., and Henningsmoen, G. (1948) Deep boring through Ordovician and Silurian strata at Kinnekulle, Västergötland: *Bull. Geol. Inst. Univ. Uppsala* **32**, 337–474.
- Watanabe, T. (1981) Identification of illite/montmorillonite interstratifications by X-ray powder diffraction: *J. Miner. Soc. Japan, Spec. Issue* **15**, 32–41 (in Japanese).
- Weaver, C. E. (1953) Mineralogy and petrology of some Ordovician K-bentonites and related limestones: *Geol. Soc. America Bull.* **64**, 921–964.
- Weaver, C. E. and Pollard, L. D. (1973) *The Chemistry of Clay Minerals*, Elsevier, Amsterdam, 250 pp.
- Weir, A. H., Ormerod, E. C., and ElMansey, I. M. I. (1975) Clay mineralogy of sediments of the western Nile delta: *Clay Miner.* **10**, 369–386.

(Received 27 June 1985; accepted 29 March 1986; Ms. 1497)